Available online at www.sciencedirect.com
SCIENCE DIRECT
Engineering Geology 82 (2006) 202–221
ENGINEERING GEOLOGY
www.elsevier.com/locate/enggeo

Geological and geomorphological characteristics of landslides triggered by the 2004 Mid Niigta prefecture earthquake in Japan

Masahiro Chigira [a,*], Hiroshi Yagi [b]

[a] Disaster Prevention Research Institute, Kyoto University Gokasho, Uji 611-0011, Japan
[b] Yamagata University 1-4-1 Koshirakawa, Yamagata 990-8560, Japan

Received 16 June 2005; received in revised form 14 October 2005; accepted 26 October 2005
Available online 27 December 2005

Abstract

The 2004 Mid Niigta prefecture earthquake (M_{JMA} 6.8) triggered more than one thousand landslides in the Miocene to Quaternary sedimentary rocks in Japan. The most common landslides were shallow disrupted landslides on steep slopes, which has been common in many previous disastrous earthquakes in the world. The Mid Niigta prefecture earthquake also triggered more than one hundred deep landslides, providing valuable information on the conditions for their occurrence. A field investigation and the interpretation of aerial photographs taken before and after the earthquake suggest that reactivation of existing landslides and undercutting of slopes are the most important factors for deep landslides to be triggered by earthquakes. In addition, planar sliding surfaces seem to be essential for the generation of catastrophic landslides triggered by this earthquake. Planar bedding–parallel sliding surfaces were formed at the boundary between the overlying permeable sandstone and underlying siltstone or along the bedding planes of alternating beds of sandstone and siltstone. Sliding surfaces along the slope-parallel oxidation front were formed in the area of black mudstone. New landslides (rockslide-avalanches) occurred with the sliding surfaces in a several-cm thick tuff interbedded in siltstone. One rockslide-avalanche occurred on a slope where buckling deformation preceded the earthquake. Gentle valley bottom sediments were mobilized in many locations, probably because they were saturated and partial liquefaction had occurred due to the earthquake shaking.

Keywords: Chuetsu; Earthquake; Landslides; Rockslide-avalanche; Geomorphology

1. Introduction

The 2004 Mid Niigta prefecture earthquake (Japan Meteorological Agency; JMA), which occurred on October 23rd, 2004 in Niigata Prefecture, central Japan, induced a large number of landslides, causing severe damage and isolating villages in the epicentral mountainous areas. Thirteen people were killed in the earthquake, six by landslides. Thirty-three more people died later because of diseases induced by the earthquake or by the aftershocks that occurred up to March 22nd, 2005. This earthquake occurred in an area with many previous landslides, and thus the area still has unstable or metastable landslide mass. This earthquake was one of the major earthquakes to give various scientific data of earthquake-induced landslides in such an area; earthquakes that induced distributed landslides in the past decade or so include the 1999 Chi-Chi earthquake in Taiwan, the 1995 Hygoken-nanbu earthquake in Japan, the 1994 Northridge earthquake and the 1989 Loma Prieta earthquake in the USA.

* Corresponding author. Tel.: +81 774 38 4100; fax: +81 774 38 4105.
E-mail address: chigira@slope.dpri.kyoto-u.ac.jp (M. Chigira).

0013-7952/$ - see front matter © 2005 Elsevier B.V. All rights reserved.
doi:10.1016/j.enggeo.2005.10.006

Landslides triggered by the 1989 Loma Prieta earthquake (Mw 6.9) have been studied by Keefer and Manson (1998), Keefer (2000), and others. One-thousand, two-hundred eighty landslides were identified and mapped (Keefer, 2000). Keefer (2000) pointed out that the geotechnical parameters of internal friction and cohesion and calculated strength at a given depth did not explain the distribution and density of landslides, and that regional-scale variations in the hazard level of seismically induced landslides might be better correlated with the lithological characteristics rather than the geotechnical parameters, which is the main theme of our paper.

Landslides induced by the 1994 Northridge earthquake (Mw 6.7) were studied by Harp and Jibson (1996) and Parise and Jibson (2000). Harp and Jibson (1996) mapped 11,000 landslides, and found that the most common types of landslides were highly disrupted, shallow falls and slides of rock or debris, with deeper, more coherent slumps and block slides occurring by the hundreds, mostly as the reactivation of previously existing landslides. However, the geologic structure of these deep landslides was not clarified. Landslides triggered by both the 1989 Loma Prieta and 1994 Northridge earthquakes had different concentrations according to geologic units and seemed to have preferential geology, but this aspect was not considered in detail by Keefer (2000) or Parise and Jibson (2000). These landslides occurred in dry areas, so the groundwater effect was probably insignificant.

Landslides triggered by the 1999 Chi-Chi earthquake (Mw7.5) have been thoroughly studied by Wang and his colleagues (Wang et al., 2002, 2003a,b; Chigira et al., 2003) and the Central Geological Survey of Taiwan (Central Geological Survey, 2000). Wang et al. (2002, 2003b) identified approximately 10,000 distributed landslides by using SPOT images, and found that the aerial rate of landslides decreases from the epicenter and the effect of rock type on the landslide rate is also significant. They reported the geologic features of deep-seated landslides (Wang et al., 2003a; Chigira et al., 2003), and the geological features of relatively small slides were reported locally in Taiwan (Central Geological Survey, 2000).

The Newmark method is one of the most important approaches for assessing earthquake-induced landslide hazard (Newmark, 1965; Wilson and Keefer, 1983). Jibson et al. (2000) applied this method to the landslides in the 1994 Northridge earthquake. The landslide probability shown by Jibson et al. (2000) seems to be consistent with the actual landslide distribution, but they did not take into account the type of landslides that occurred, so some landslides may not be related to this probability.

As described above, the geologic characterization of landslides triggered by earthquakes is fatally insufficient, particularly for rather small landslides, despite the fact that statistical analyses of landslides have been performed by many researchers. Distributed landslides triggered by earthquakes have been studied statistically, but the geologic structures of deep landslides have not been studied sufficiently, except for exceptionally large landslides, although deep landslides probably have structural causes. Gigantic landslides studied in detail include the Madison canyon landslide in the USA (Hadley, 1964), Nevados Huas caran in Peru (Plafker et al., 1971), Chiu-fen-erh-shan and Tsaoling in Taiwan (Chigira et al., 2003; Wang et al., 2003a), Bairaman in Papua New Guinea (King et al., 1989), the Ontake kuzure in Japan (Endo et al., 1989; Kobayashi et al., 1991; Voight and Sousa, 1994), and Turnagain Heights in the USA (Hansen, 1965; Seed and Wilson, 1967). Keefer (1984a) analyzed data from 40 historical world wide earthquakes, and obtained the relationship between the maximum distances of landslides from the epicenter or fault rupture for each type of landslides, but did not examine detailed geologic structures. Rodriguez et al. (1999) added data on 36 earthquakes since 1980 to those studied by Keefer (1984a), and obtained results similar to Keefer (1984a), with some exceptions. Keefer (1984a,b) summarized the source characteristics of rock avalanches caused by earthquakes, and found that the height, inclination, and undercut condition of slopes are the most important factors for their generation, although he also mentioned that site-specific geologic conditions are also important.

This paper reports and discusses the basic causes and mechanisms of the deep landslides triggered by the 2004 Mid Niigta prefecture earthquake. A detailed distribution of the landslides was plotted by the Japan Geographical Institute (2004) immediately after the earthquake, and was published as a 1:30,000 scale map, which counted 1353 landslides and greatly contributed to the recovery strategy from the disaster. Yagi et al. (2004) interpreted the aerial photographs taken by the Aero Asahi Corporation on October 28th, 2004 with a scale of 1:10,000, and plotted landslides and cracks on a detailed map that was made using an airborne laser scanner. We interpreted aerial photographs taken before and just after the earthquakes and conducted a field investigation: aerial photographs with a scale of 1:10,000 taken October 24th, 2004 by the Kokusai Kogyo Company and aerial photographs with a scale of 1:10,000 taken in 1975 and 1976 by the Japan

Geographical Institute. Our geological field investigation was conducted for two weeks, and clarified the geologic structures of major landslides. We obtained numerical data on the scale of the landslides from the digital elevation model with a 1-m grid made by an airborne laser scanner (Yagi et al., 2004).

2. Geological setting and earthquake characteristics

The epicentral area is located in the Higashiyama Hills and its neighboring alluvial plain, where the Shinano River flows from SW to NE then turns to NW to N after merging with the Uono River (Fig. 1). The Higashiyama Hills is northeast of the rivers. The elevation of the river near the Hills is 50–80 m, and the summit levels of the Higashiyama Hills range from 400 to 700 m. The central part of the Hills is cut by the Imo River flowing from north to south.

The geological outline is summarized as follows from Yanagisawa et al. (1986) and Kobayashi (1987) (Fig. 2). The Higashiyama Hills is underlain by Miocene to Pleistocene strata, which trend NNE–SSW with several anticlines and synclines. Where the fold axes plunge, the trend of the strata changes to E–W locally. The axes are named the Higashiyama anticline, Konpira syncline, Toge anticline, Kajikane syncline, and Komatsugura anticline from the west to the east with a half wavelength of about 1 km (Fig. 2). The strata consist mainly of mudstone, alternating beds of siltstone and sandstone, and sandstone with subordinate dacitic or andesitic volcanic rocks. The formations shown in Fig. 2 are these volcanic rocks, thick mudstones – the Araya and the Ushigakubi Formations–, and a thick sandstone — the Wanatsu Formation; other areas in white in Fig. 2 mostly consist of the alternating beds of sandstone and siltstone. The volcanic rocks and the Araya Formation are Miocene in age, and the strata above it up through the Wanatsu Formation are of Pliocene age. The strata above the Wanatsu Formation are Quaternary. The Araya and the Ushigakubi Formations consist mainly of mudstone, but contain sandstone beds near the boundaries with other formations that consist of alternating beds of sandstone and siltstone.

The Higashiyama Hills and the surrounding area are tectonically active with some active faults and active folds, of which the nearest one from the epicenter is the Yukyuzan fault west of the Higashiyama Hills (Research Group for Active Faults of Japan, 1991).

The mainshock of the 2004 Mid Niigta prefecture earthquake (M6.8) occurred at 5:56 PM (Japan Standard Time) on October 23rd, 2004, with a local body wave magnitude (M_{JMA}) of 6.8 and with many aftershocks (Table 1); three of the aftershocks exceeded magnitude 6. The hypocenter of the main shock was

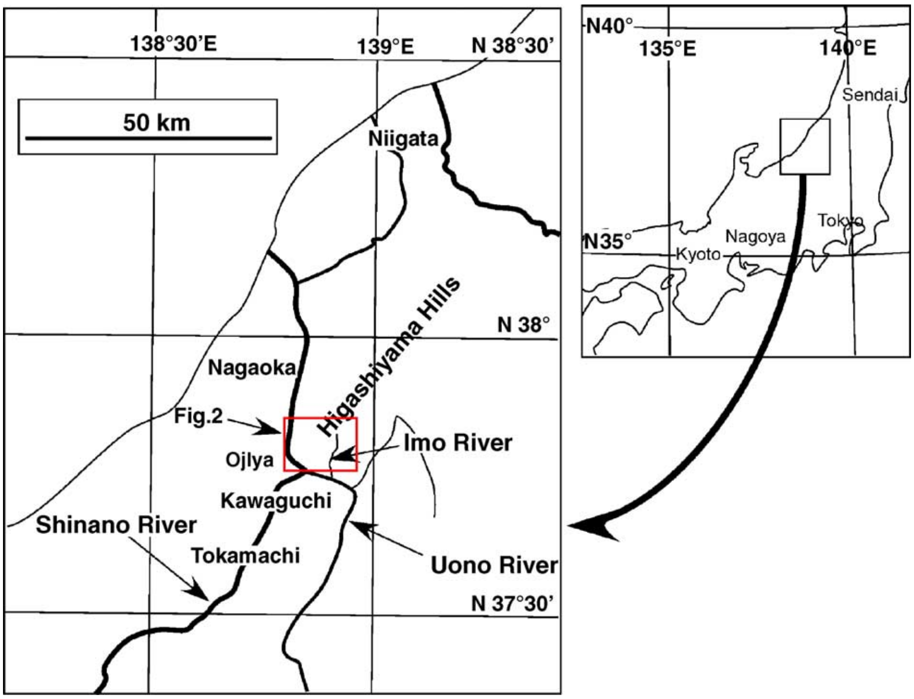

Fig. 1. Index map.

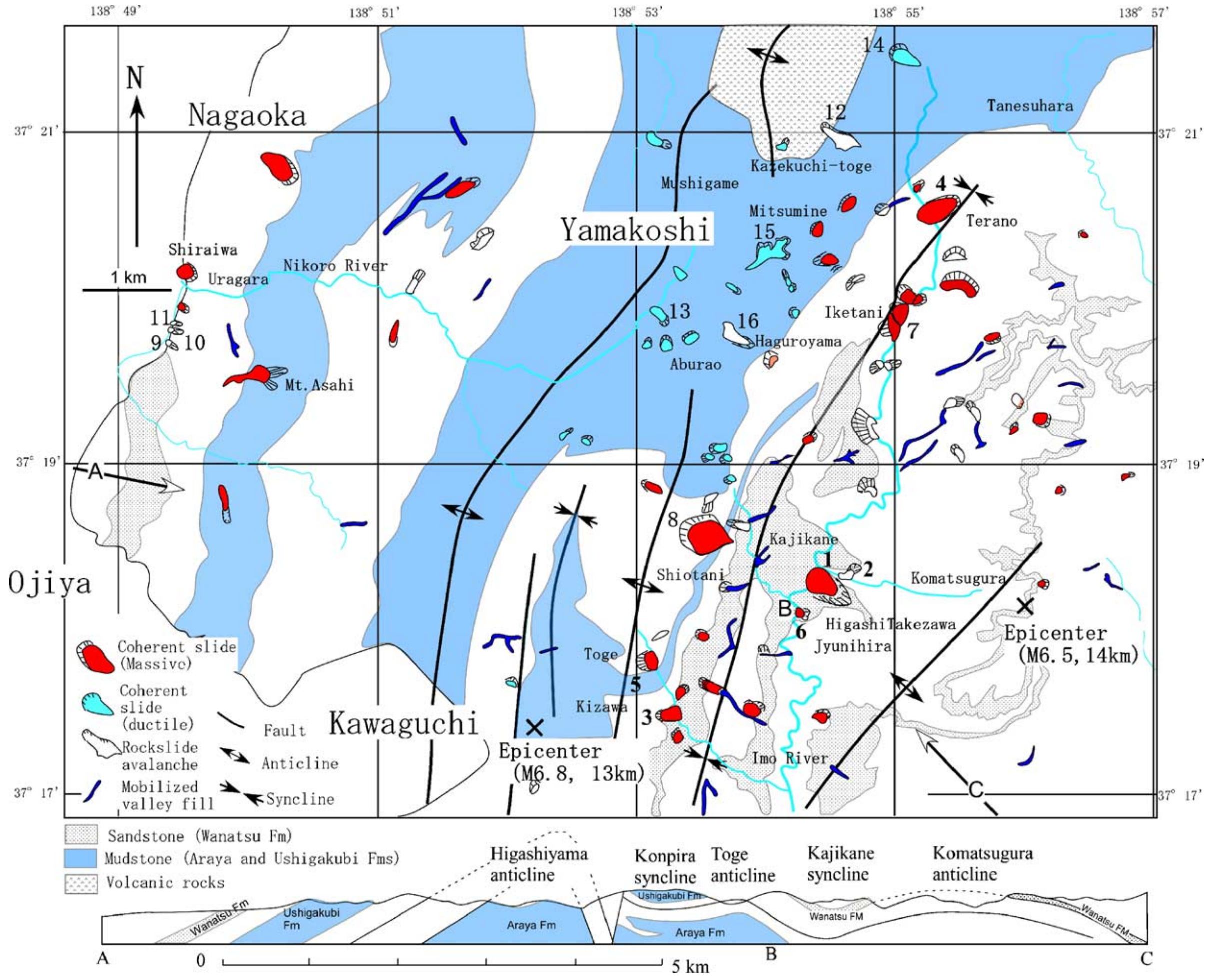

Fig. 2. Geologic outline and the distribution of major landslides in the Higashiyama Hills. Geologic outline is modified from Yanagisawa et al. (1986) and Kobayashi et al. (1991).

13 km below Kawaguchi town (Fig. 2). An aftershock occurring at 6:34 PM on 23rd was 14 km deep to the east of Komatsugura. Analyses of the aftershock distribution and geodetic modeling by several investigators showed that several faults ruptured sequentially. The rupture fault surfaces of the main shock provided by the Geographical Survey Institute and that by the Earthquake Research Institute at the University of Tokyo differed slightly, but both showed a trend NE–SW and a dip westward. The rupture fault was a thrust with a maximum compression axis of WNW–ESE, which is a common type observed around this area (Japan Meteorological Agency web site accessed on March 29th, 2005). The maximum accelerations in the Higashiyama Hills were 1722 gals (N–S: 1142; E–W: 1675; vertical: 870) at Kawaguchi, 1131 gals (N–S: 538; E–W: 722; vertical: 1059) at Yamakoshi, and 1008 gals (N–S:779; E–W: 898; vertical: 731) at Ojiya, respectively.

3. Distribution and type of landslides

Many landslides occurred in a wide area on the Higashiyama Hills, and were particularly dense along the Imo River and Kajikane syncline (Fig. 2). This dense area seems to have experienced the most intense earthquake tremors, because almost all of the houses within this area collapsed or sustained severe damage. Gigantic landslides did not occur, as will be discussed later, but relatively small landslides dammed rivers to make landslide dams in more than 30 locations (The Geographical Survey Institute, 2004); two landslide dams were much bigger than the others, and the lakes that formed were drained immediately to prevent flooding upstream and downstream.

We extracted major landslides wider than 20 m or longer than about 100 m and deeper than about 5 m from the interpretation of the aerial photographs; the

Table 1
List of the main shock and aftershocks (from October 23rd to November 8th, 2004)

Date	Latitude (N)	Longitude (E)	MJMA	Depth (km)	Maximum intensity (JMA scale)	Maximum acceleration (gals)
17 h 56 m 23, Oct	37° 17.4′	138° 52.2′	6.8	13	7	1722 (Kawaguchi) 1131 (Yamakoshi) 1008 (Ojiya)
17 h 59 m 23, Oct,	37° 18.6′	138° 51.5′	5.3	16	5+	
18 h 03 m 23, Oct	37° 21.1′	138° 59.2′	6.3	9	5+	
18 h 07 m 23, Oct	37° 20.7′	138° 52.1′	5.7	15	5+	
18 h 11 m 23, Oct	37° 15.0′	138° 50.0′	6	12	6+	841 (Ojiya)
18 h 34 m 23, Oct	37° 18.2′	138° 56.0′	6.5	14	6+	2515 (Kawaguchi) 770 (Ojiya)
18 h 36 m 23, Oct	37° 15.2′	138° 56.7′	5.1	7	5−	
18 h 57 m 23, Oct	37° 12.2′	138° 52.0′	5.3	8	5+	
19 h 36 m 23, Oct	37° 12.8′	138° 49.7′	5.3	11	5−	
19 h 45 m 23, Oct	37° 17.6′	138° 52.8′	5.7	12	6−	
19 h 48 m 23, Oct	37° 17.7′	138° 50.4′	4.4	14	5−	
14 h 21 m 24, Oct	37° 14.5′	138° 49.8′	5	11	5+	
0 h 28 m 25, Oct	37° 12.0′	138° 52.4′	5.3	10	5−	
6 h 04 m 25, Oct	37° 19.6′	138° 57.0′	5.8	15	5+	
10 h 40 m 27, Oct	37° 17.3′	139° 02.2′	6.1	12	6−	392 (Ojiya)
8 h 57 m 04, Nov	37° 25.6′	138° 55.1′	5.2	18	5+	
11 h 15 m 08, Nov	37° 23.5′	139° 02.1′	5.9	very shallow	5+	

Preliminary data reported on the web site of the Japan Meteorological Agency accessed on March 29th, 2005. Maximum accelerations in the study site were selected from the data (Kawaguchi, Yamakoshi, and Ojiya).

total number of these landslides was about 100. The landslides, except for shallow disrupted landslides, are classified as follows:

- Coherent landslide
- Rockslide avalanche
- Mobilization of valley fill.

This classification is about the same as those by Sato et al. (2004) on the basis of the Geographical Survey Institute (2004) and by Yagi et al. (2004), although their classifications are more detailed. A coherent landslide corresponds to the Category II slide (*Jisuberi* in Japanese), and shallow disrupted landslide and the rockslide avalanche (*Houkai* in Japanese) probably correspond to the Category I slide of Keefer (1984a, 2000). Besides these, flash floods from the breach of ponds used to breed golden carps occurred, washing out surface sediments like debris flow.

The schematic sketches of landslides are shown in Fig. 3. Numbers 1 to 5 correspond to coherent landslides, numbers 6 and 7 to rockslide avalanches, and number 8 to mobilization of valley fill. Their characteristics will be described in the following sections. Coherent landslides will be described first according to geology: landslide of sandstone on siltstone, landslide of alternating beds of sandstone and siltstone, and landslide of weathered mudstone. Numerical data of the landslides described in the following sections are summarized in Table 2.

3.1. Landslide of sandstone on siltstone

Many landslides occurred along the base of a thick sandstone bed, which belongs to the Pliocene Wanatsu Formation of Yanagisawa et al. (1986) (Fig. 2); it is underlain by siltstone or the alternating beds of siltstone and sandstone of the Pliocene Shiraiwa Formation. A typical landslide of this type was the Higashi-Takezawa slide (Type 1 in Fig. 3, Loc. 1 in Fig. 2), which blocked the Imo River, making a pond and flooding a small village upstream. This landslide was a partial reactivation of an existing old landslide (Fig. 4). The old landslide was on a northwestward-facing slope with a U-shaped scarp apex towards the southeast and a U-shaped depression just below the scarp. The landslide mass downslope of the depression was 350 m long and had a maximum width of 300 m. Although the foot of the slide mass was cut by the Imo River, forming a steep slope before the earthquake, a mound on the opposite side of the river indicates that the landslide once dammed the river and then was later eroded by the river (Figs. 4 and 5). This landslide mass was also eroded at its southwestern side by a linear gully from the Imo River reaching to the depression.

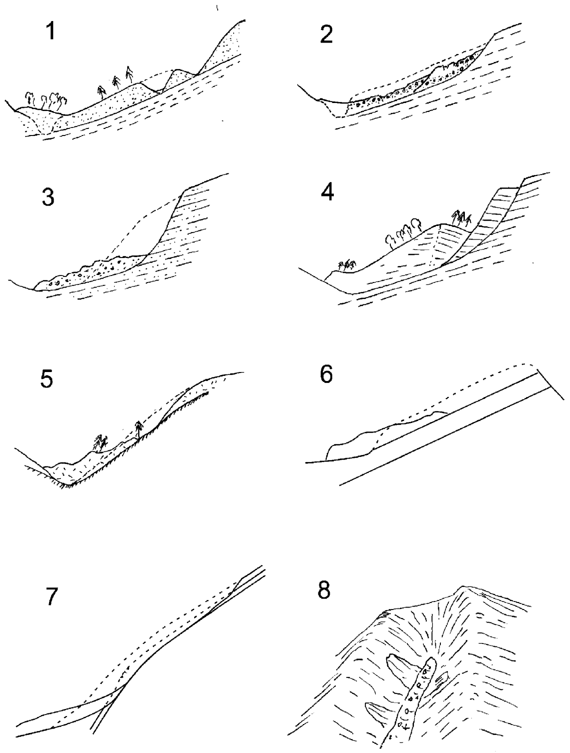

Fig. 3. Types of landslides. Corresponding numbers are explained in the text as well as Table 2.

The landslide induced by the Mid Niigta prefecture earthquake involved the main part of the old slide mass, but its uppermost parts and leftmost parts (to the south of the small gully) did not slide. Upslope from the head of the slid mass a sliding surface was exposed along the top of the siltstone bed below the sandstone that slid (Fig. 6). The mass of sandstone that slid was estimated to be about 20 m thick, and its volume was estimated to be about 2 million m^3, judging from the map made by the airborn laser altimetry (Yagi et al., 2004). The top of the siltstone below the sandstone was also exposed at the bottom of the old landslide scarp (Fig. 5). A spring was always observed along the boundary between the sandstone bed and the underlying siltstone bed in November. The bedding plane was very planar and dipped northwestward at 20°. On the slip surface exposed this time, we found films of limonite, many of which were fragmented and dispersed on the surface but were lithified (Fig. 6). This fact strongly indicates that limonite films, which were made on top of the impermeable siltstone below the permeable and oxidized sandstone, were broken by the old landslide, and then lithified, and exposed by the landslide during the Mid Niigta prefecture earthquake. From the morphology of the new slide, the mass slid translationally without rotation first, and then climbed up the opposite slope, being rotated backward at its toe. The apparent friction angle, which is an inclination of a line connecting the top and the distal end of a landslide, was as small as 8°.

From the geologic structure and the existence of springs along the top of the siltstone bed, the overlying sandstone was assumed to be saturated with water before the earthquake. In addition, three to two days before the earthquake, there was precipitation of about 100 mm, which was observed at Tochio, 20 km to the north of this site, and this probably elevated the groundwater table within the slide mass. The pore pressure exerted by the groundwater and the earthquake tremor triggered the landslide. The reason why the uppermost and left part of the old slide mass did not slide may be due to the drainage along the U-shaped depression and a gully.

The combination of this sandstone and the underlying siltstone was traceable to the northeast, where another slide (Loc. 2 in Fig. 2) occurred. The Kizawa East slide (Loc. 3 in Fig. 2) was also a slide of the sandstone on siltstone, where an arcuate head scarplet was observed on aerial photographs before the earthquake.

3.2. Landslide of alternating beds of sandstone and siltstone

3.2.1. Landslide with ridges and grabens (Type 2 in Fig. 3)

Ridges and grabens were made by the Terano slide (Loc. 4 in Figs. 2 and 7), which was a reactivated landslide, that dammed the Imo River. The surface of the pre-earthquake slide gently inclined to the SW with an 8-m high landslide scarp and a steep toe, which was made by the erosion by the Imo River (Fig. 7). This previous landslide mass was 140 m wide and 300 m long with a relatively smooth surface. Before the earthquake, the width of the Imo River was much narrower at the foot of the landslide than upstream and downstream. This indicates that the landslide used to dam the Imo River, and later was eroded by the river at the foot, being destabilized before the Mid Niigta prefecture earthquake, which triggered the landslide and dammed the river again.

This landslide is located at the axial part of the SSW-plunging Kajikane Syncline (Fig. 2). The strata underlying the landslide consist of alternating beds of sandstone and siltstone, which are dominated by sandstone. The bedding plane trends WNW and dips 12 to 14° SSW. The landslide slope, therefore, is approximately a dip slope, dipping to the direction with an angle of 60° with the dip direction of the bedding plane. The strata excavated and exposed within the landslide retained their original structure from before this earthquake

Table 2
List of the landslides studied in detail

Type		Location Numbers are shown in Fig. 2	Lithology	Bedding dip (°)	Angle between the dip directions of beds and slope (°)	Sliding surface	Downslope condition	Reactivation or new	Total length (m)	width (m)	Total area (*10^{3}m^2)	Estimated thickness (m)	Estimated volume (*10^{3}m^3)	Crown elevation (m)	Toe elevation (m)	Apparent friction angle (°)
Coherent slide	1	Higashi Takezawa (1)	Ss/Sils	20	0	Ss/Sils	Undercut	React.	470	210	99	20	2,020	224	160	8
		Higashi Takezawa (2)	Ss/Sils	22	60	Ss/Sils	Undercut	React	280	30	8	4	30	238	154	17
		Kizawa (3)	Ss/Sils	42	45	Ss/Sils	Unknown	React.	260	130	34	8	170	250	150	21
	2	Terano (4)	Altn Ss-Sils	14	50	Bedding	Undercut	React.	390	160	62	10	510	314	248	10
	3	Toge (5)	Altn Ss-Sils	12	30	Bedding?	Undercut?	React.	330	200	66	5	220	264	168	16
		Jyunihira (6)	Altn Ss-Sils	14	30	Bedding	Undercut	Unknown	260	200	52	4	160	240	188	11
		Iketani (7)	Altn Ss-Sils	10	90	Bedding	Undercut	React.	180	210	38	12	270	238	198	13
	4	Shiotani (8)	Altn Ss-Sils	14	40	Bedding	Undercut	React.	740	470	348	30	5,370	350	162	14
	5	Aburao (13)	Ms	–	–	Oxidation front	Undercut	React.	240	110	26	4	60	238	166	17
		Tanesuhara (14)	Ms	–	–	Oxidation front	Undercut?	React.	290	180	52	4	80	396	312	16
		Mitsumine (15)	Ms	–	–	Oxidation front?	Unknown	React.	400	100	40	3	60	370	258	16
Rockslide avalance	6	Shiraiwa (9)	Sils with tuff	22	6	Debris/Sils (tuff)	Undercut (road)	React.	90	30	3	4	7	70	46	14
		Shiraiwa (10)	Sils with tuff	22	6	Tuff	Undercut (road)	New	60	50	8	3	10	89	46	15
		Shiraiwa (11)	Sils with tuff	22	6	Tuff	Undercut (road)	New	120	40	5	3	6	78	42	17
	7	Kazekuchitoge(12)	Sils	30–42	26	Bedding	Buckling	Inside a previous scar	520	90	47	4	90	470	284	20
	Others	Haguroyama (16)	Ss/Ms	Unknown	Unknown	Joint or fault	Undercut?	Unknown	450	60	27	3	30	422	230	23

which was already disturbed; the siltstone was brecciated and its blocks floated in loose fine sand owing to the previous landslide.

The landslide triggered by the earthquake extended the existing main scarp, formed a subsidiary scarp in the middle, and made small ridges and grabens, a few meters to 10 m wide, although essentially no rotation was observed (Fig. 7). The right and left flank scarps had different heights; the right (NW) scarp decreased in height downslope and disappeared at the middle, while the left scarp was as high as 8 m from the headscarp to near the toe. This may be due to the fact that the strike of the bedding plane was slightly oblique to the strike of the slope and daylighted at the NW side of the landslide. These morphological features and the geologic structure mentioned before indicate that the slide occurred translationally along planar bedding planes. The depth of the slide is estimated to be about 10 m, based on preliminary information from drilling performed in the middle of the landslide.

The toe of the landslide was immediately excavated to drain the dammed river, and the base of the landslide debris was exposed on the solid bedrock; groundwater was being discharged from this boundary. This fact and the fact that the landslide mass consisted of siltstone blocks floating in loose fine sand indicate that pore pressure reduced the effective stress and possibly some liquefaction occurred.

3.2.2. Landslide with lateral spreading at lower part of a slope and settlement of upper part (Type 3 in Fig. 3)

Several landslides with an extraordinarily high landslide scarp occurred, which the Iketani slide exemplifies (Loc.7 in Figs. 2 and 8). This slide is located near the axis of the Kajikane Syncline, and the beds had trends E–W and dips 10° southward. The bedding plane is apparently horizontal in E–W cross-section, which was the movement direction of the slide. Comparison between the aerial photographs before and after the earthquake (Fig. 8) indicated that the upper part of the slide mass settled about 30 m with very small backward rotation (less than 10°) and the lower part moved laterally with pressure ridges (Fig. 9A). The slide mass consisted of alternating beds of siltstone and sandstone. A sliding zone observed at the downslope edge of this slide mass was about 30 cm thick and consisted of clay containing silt, sand, and fragments of siltstone and tree trunks, sandwiched between the underlying river gravel and overlying alternating beds of sandstone and siltstone (Figs. 9B and 9C). This slide is inferred to have occurred by the lateral spreading of the lower part of the slope along the bedding plane due to

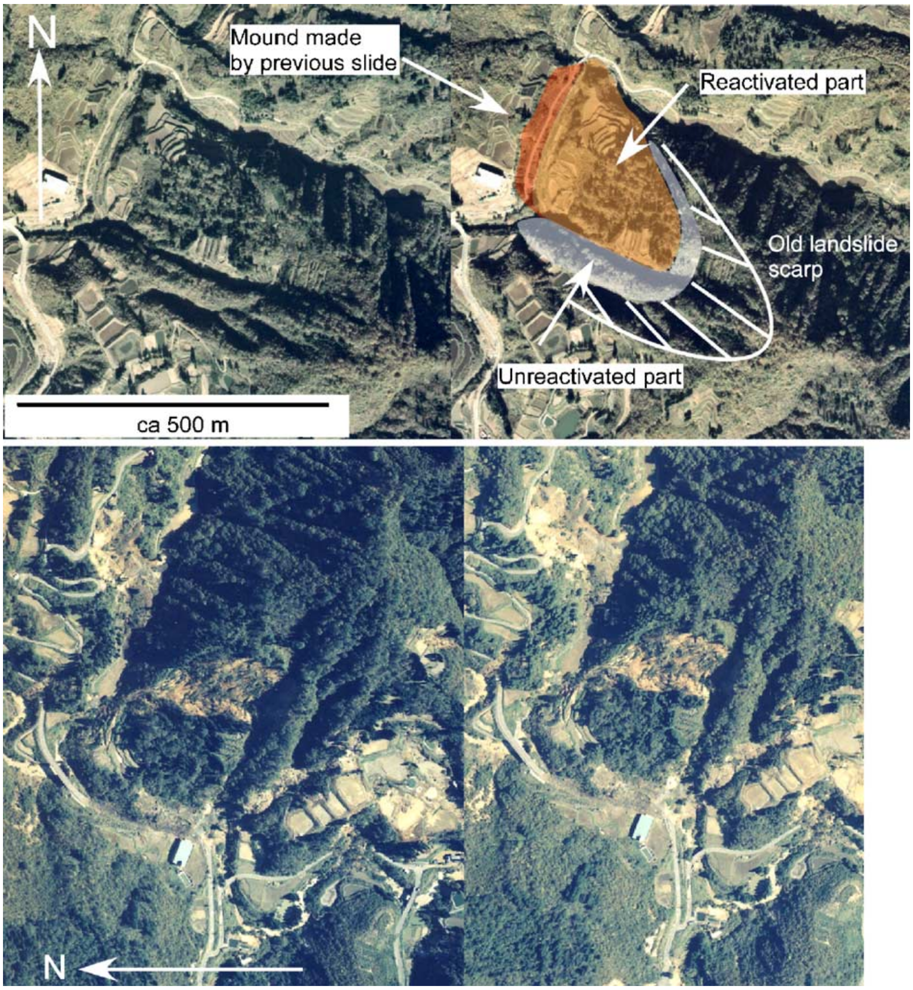

Fig. 4. Aerial photographs before (above) and after (below) the slide of the Higashi-Takezawa slide. The reactivated portion is indicated. The photographs before the earthquake taken by the Geographical Survey Institute (Photo numbers: ccb-76-3-c3-34, 35). The photographs after the earthquake taken by the Kokusai Kogyo Co (C-4, 4128, 4129).

intense earthquake shaking and by the subsequent settlement of the upslope part, leaving a large scarp. The aerial photographs beore the earthquake indicated that this slide was a reactivation of the distal part of a previous landslide, which came from the east to block the Imo River once and later dissected by erosion.

Landslides with a large head scarp occurred in other locations within the area of alternating beds of sand-

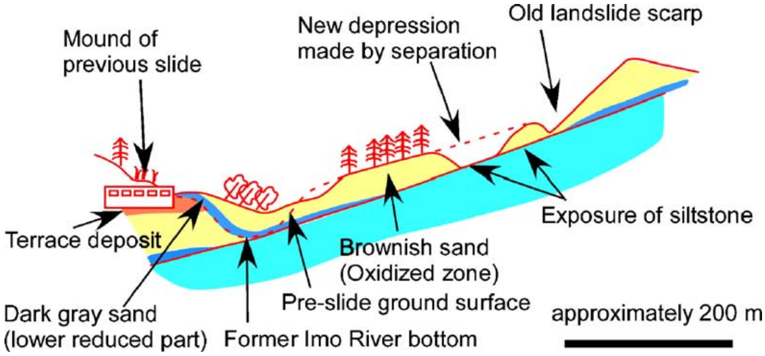

Fig. 5. Schematic cross-section of the Higashi-Takezawa slide.

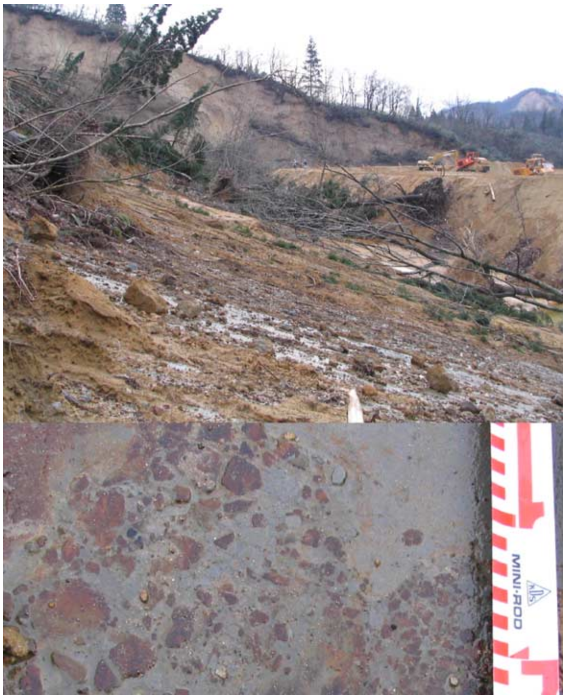

Fig. 6. Planar sliding surface of the Higashi-Takezawa slide and brecciated limonite film on the sliding surface. The scale in the lower photograph is 10 cm.

stone and siltstone, including Toge slide (Loc. 5 in Fig. 2).

3.2.3. Landslide with a "roll-over" antiform on the rear side. (Type 4 in Fig. 3)

A "roll-over antiform" was observed for the Shiotani landslide (Loc. 8 in Fig. 2), which was the largest slide triggered by the Mid Niigta prefecture Earthquake: 470 m wide and 740 m long with a 30-m high landslide scarp (Fig. 10). This slide was also due to reactivation of a previously existing slide. This slide occurred on the southeastern slope of a 400-m high mountain. This slope was between an east-trending ridge and a south-trending ridge; an arcuate landslide scarp had been made upslope before the earthquake.

The geologic map of Yanagisawa et al. (1986) indicates that this locality is on the eastern limb of the south-plunging Toge Anticline (Fig. 2). The strata observed to the west of the slide trend NNW and dip 14° eastward, but they are inferred to have northeastern trend under the slide area because the anticlinal axis plunges southward.The aerial photographs taken before and after the earthquake showed that the uppermost part of the previous landslide was not reactivated. The ground surface of the reactivated part rotated backward 30° at its head,

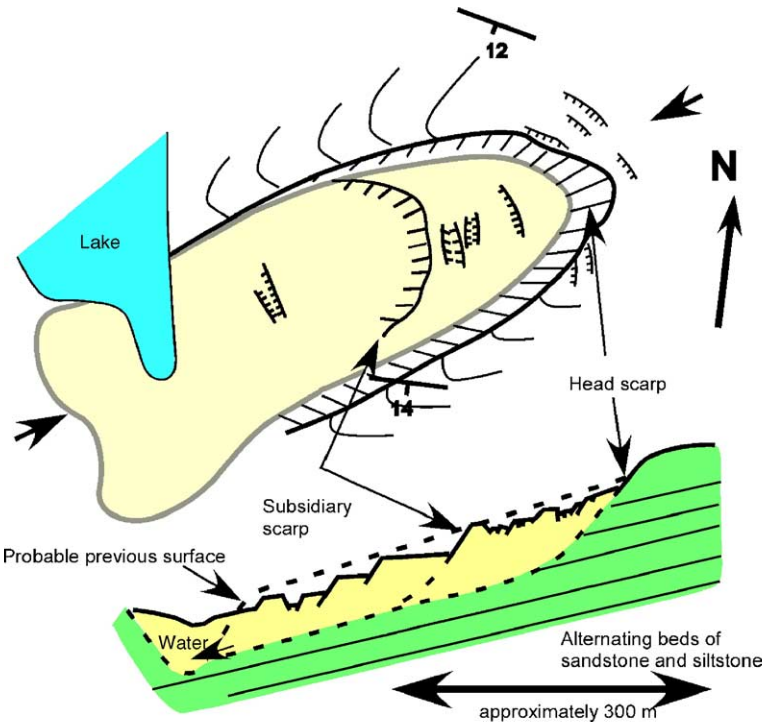

Fig. 7. Schematic plan sketch and cross-section of the Terano slide.

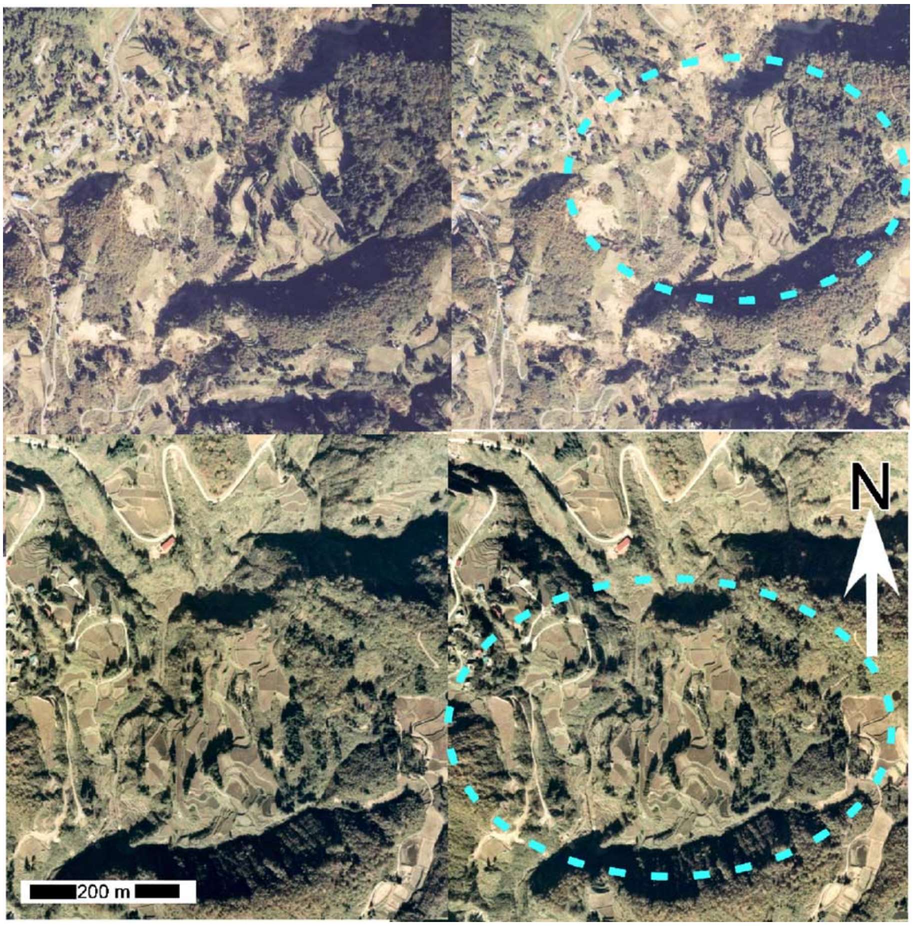

Fig. 8. Stereopairs of aerial photographs of Iketani slide before (below) and after the earthquake (above). Above photographs were taken by the Aero Asahi Corporation and the photographs below were by the Geographical Survey Institute (photo numbers: CCB-76-3,C1-34,35). The Iketani slide moved by the earthquake is on the western side of the river. The whole area of previous slide, which slid westward once blocked the river. And later eroded, is encircled.

but did not rotate in the middle, judging from the tree attitudes (Fig. 10). The toe of the slide overrode the opposite slope and rotated 25° backward. These ground surface attitudes indicate that the slip surface in the middle and lower part of the slope was planar and parallel to the bedding plane, and listric upslope. The strata above the listric slip surface rotated backward, forming a "roll-over" antiform in a manner similar to that shown by Ramsay and Huber (1987){Ramsay, 1987 #58}{Ramsay, 1987 #58}{Ramsay, 1987 #58}{Ramsay, 1987 #58}. The bedding plane exposed at the landslide scar dipped 20° to the west, which was the result of the backward rotation of the previous landslide.

3.3. Landslide of weathered mudstone (Type 5 in Fig. 3)

Reactivation of weathered mudstone slides occurred in about 20 locations in the mudstone area of the Pliocene Araya Formation (Fig. 2); many of them were oxidized mudstone slides, exposing unoxidized black mudstone on their landslide scars (Fig. 11). The surface morphology of many of the landslides occurring in the mudstone area showed ductile deformation with fewer large open cracks; this is probably due to the weakness of the weathered (oxidized) mudstone. The black mudstone exposed in the scars was just beneath the oxidation front, and was probably the dissolved and deteriorated zone reported by Chigira (1990). This indicates that the sliding surfaces were made along or beneath the oxidation front, which is common for landslides induced by artificial excavation (Chigira, 1990). The landslides listed in Table 2 include the Aburao, Tanesuhara, and Mitsumine landslides, all of which seem to have been undercut by erosion before the earthquake, based on the examination of aerial photographs. The sliding surfaces of this type of landslide

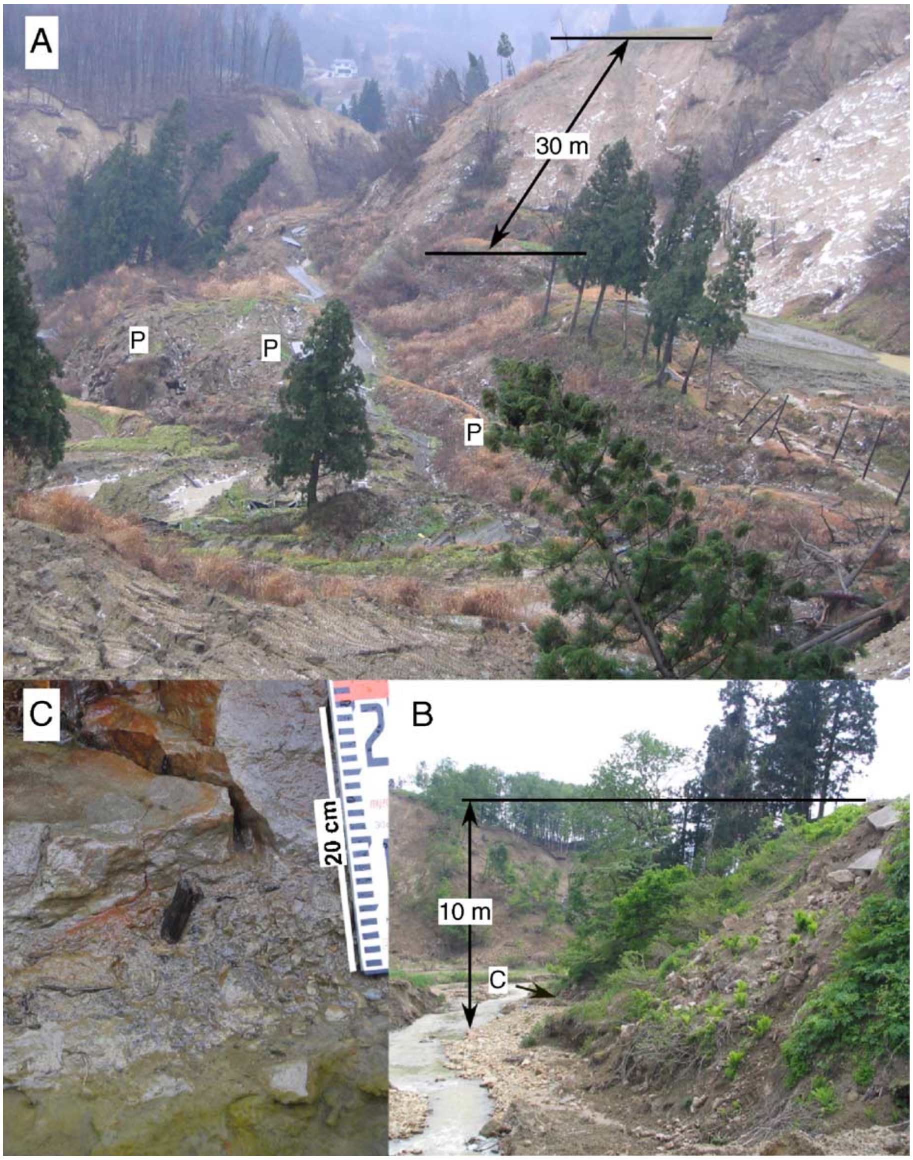

Fig. 9. The Iketani slide. A: Overview looking to the south. B: Downslope part of the slide. Looking to the south. P indicates a pressure ridge. C: Sliding zone bearing plant fragments.

may not be planar, but are inferred to be nearly parallel to the slope surface because the oxidation front is made by the downward migration of oxidizing water Chigira (1990).

3.4. Rockslide-avalanche

3.4.1. Primary rockslide with a sliding surface in a thin tuff bed (Type 6 in Fig. 3, Locs. 10 and 11 in Fig. 2)

This type of rockslide occurred in more than two locations along the western margin of the Higashiyama Hills. Figs. 12 and 13 show the photographs, geologic sketch map, and a cross-section of two of the rockslides and a neighboring debris slide. The strata here, the Shiraiwa Formation, mainly consists of siltstone, which intercalates white tuff beds of about 5 cm thickness. The sliding surface was within these tuff beds. The tuff consists of alternating laminae of medium to coarse sand-size grains and laminae of fine tuff (Fig. 12). The sand-size tuff originates from pumice fragments and is highly porous, as observed under a microscope. The tuff consists mainly of smectite, quartz, and plagioclase, which were identified by using X-ray diffraction analysis.

Fig. 10. Shiotani slide. Above: overview; below: side-looking view. The arrows indicate rotational and translational movements.

The rockslides were 40 to 50 m wide, 120 to 160 m long, and about 5 to 8 m deep. The rockslides transformed to an avalanche and made deposits at the foot of the source area. Almost no debris remained in the source area, and a very planar sliding surface was exposed there (Fig. 12). The slid strata were cut at their foot along a road before the earthquake; a few-meters-high cut slope excavated in the siltstone below the tuff remained along the lower margin of the source areas after the earthquake. The bedding plane, which dips 22°, was nearly parallel to the slope, but its trend slightly intersected the trend of the slope, as is shown in Fig. 13. Consequently, the tuff bed in which the sliding surface was formed daylighted at the downslope, right margin, and upslope (opposite side of the ridge). The tuff is very weak and could be easily broken by hand, and also absorbed a great amount of water because it consisted of porous material. The southern or left margins of the two slides were both bounded by E–W trending high-angle joints.

The debris slide located to the south of these two rockslides was part of a previous landslide (Fig. 13), where the landslide surface was parallel to the bedding and along the boundary between the surface debris and underlying siltstone. However, we found many burrows filled with white tuff on the sliding surface, which indicates that white tuff was on the siltstone and suggests that the previous slide occurred with its sliding surface along this tuff bed.

3.4.2. Landslide evolved from buckling (Type 7 in Fig. 3, Loc. 12 in Fig. 2)

This type of landslide occurred in the northern part of the study area, on the southeastern slope of a NNE–SSW trending ridge. Along the southeastern foot of the ridge, a very clear knickline was observed (Fig. 14); the upper slope inclined about 45° and the lower slope 25°. Aerial photographs taken before the earthquake showed that this slide occurred in a previous landslide scar. The underlying strata consist mainly of siltstone and prob-

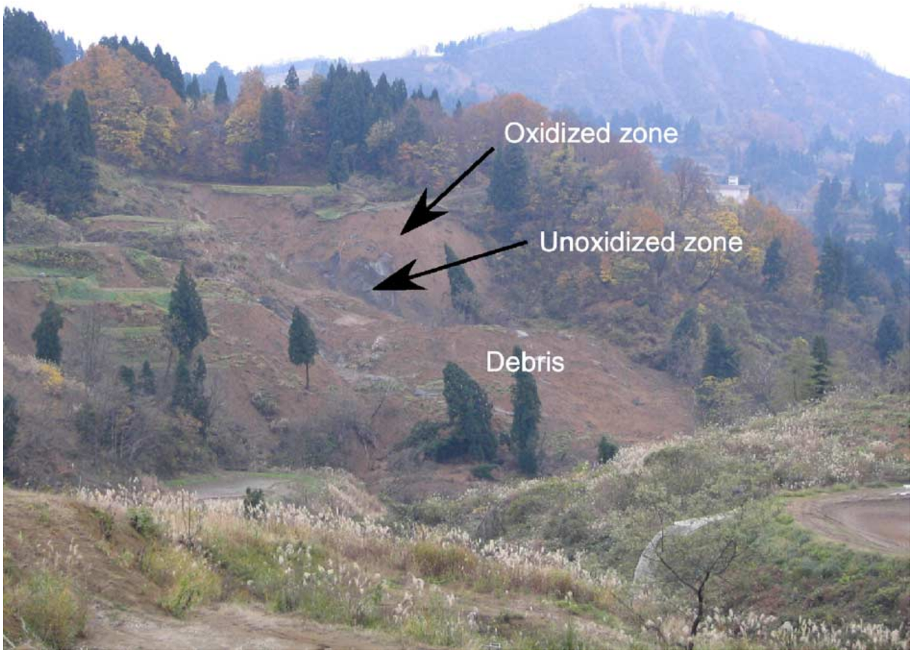

Fig. 11. Aburao slide (Number 13 in Fig. 2). Black mudstone can be seen in the middle and lower part of the landslide scarp.

ably lapilli tuff which was found in the debris. The stratification trends N45° to 55° E and dips to the east, crossing the trend of the slope (N40° E). The dip was 30° in the upper slope and 42° in the lower, forming a convex profile. Joints with an attitude of N65° E/70° W developed with intervals of 5 to 30 cm. At the north-eastern part of the scar, we observed rock plates, which were separated by bedding planes and high angle joints, overthrust on the downslope plates with a separation of 3 cm (Fig. 14); beneath these overthrusting plates were grass roots. These findings indicate that creep movement with buckling preceded the earthquake-induced landslide and the earthquake broke the buckled part of beds.

3.5. *Mobilization of valley fill (Type 8 in Fig. 3)*

Sediments, which filled gentle valleys, were mobilized in about 30 locations (Figs. 2 and 15), damaging roads or paddy fields that crossed or were located on valley bottoms. This mobilization seemed to be due to the groundwater in sediments, which were shaken by

Fig. 12. Rockslide near Shiraiwa, showing very planar sliding surface (left) and a tuff bed in which the sliding surface was made (right). Northernmost landslide in Fig. 13. Water was filtrating out of this tuff bed.

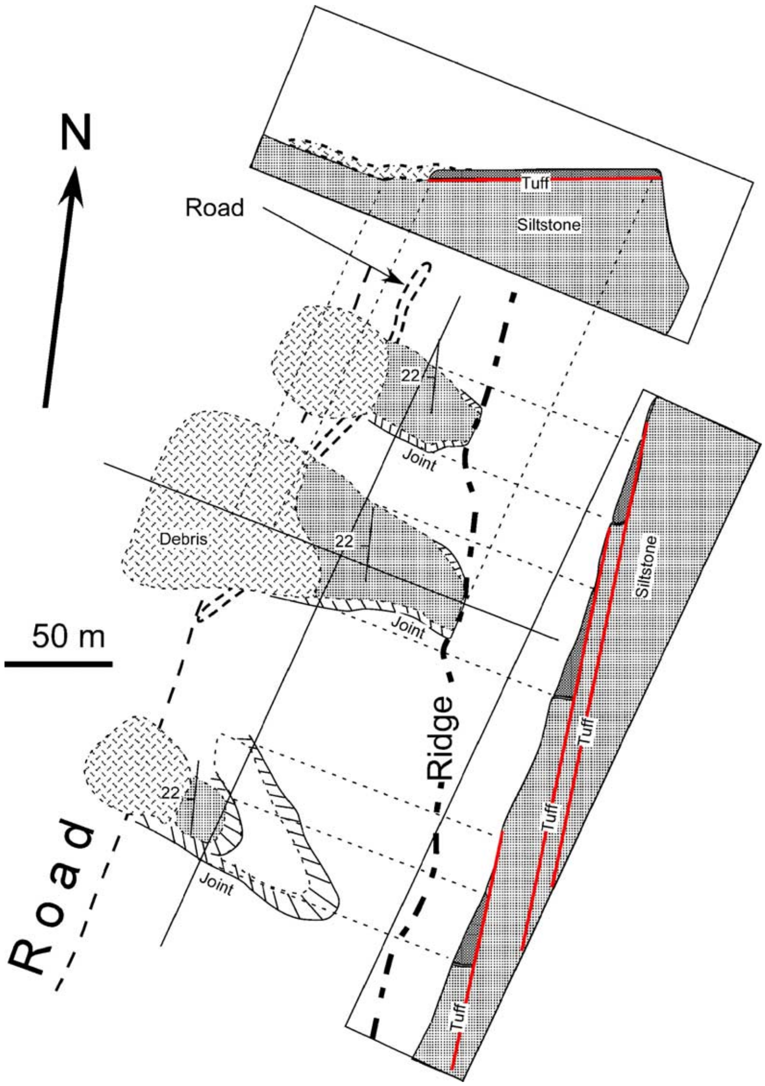

Fig. 13. Geologic sketch map of the rockslides near Shiraiwa. The southernmost one is a reactivated debris slide.

the earthquakes and probably partially liquefied. Possible liquefaction is supported by muddy sand blows sometimes observed on mobilized sediments (Fig. 15). Closely inspecting Fig. 2, we know that most mobilization of valley fill occurred in the areas of sandstone and alternating beds of sandstone and mudstone; very few valley fill mobilizations occurred in the area of mudstone, even though many landslides of weathered mudstone occurred in Yamakoshi Village, as stated before. The inclinations and intervals of the valleys, in which sediments were mobilized, are plotted in Fig. 16; they occurred in gentle valleys inclining 5° to 18°, and many of them exceeded 100 m, with two being nearly 1000 m in length. The actual movement distances are not yet known. The widths of the mobilized sediments were from 10 to 30 m. These numerical data were obtained from the map made by an air-born laser scanner (Yagi et al., 2004). The valleys where mobilization occurred, were preferentially oriented as is shown in Fig. 16: many mobilizations occurred in the valleys descending SW or W. This could be related to the earthquake shaking. However, four earthquakes with magnitudes of 6, or larger occurred within 30 min in the dark, so it is difficult to determine which earthquake triggered mobilizations.

4. Causes and mobility of landslides triggered by the Mid Niigta prefecture earthquake

The findings of the Mid Niigta prefecture earthquake indicate that undercutting condition of slopes is important for earthquakes to trigger catastrophic existing or

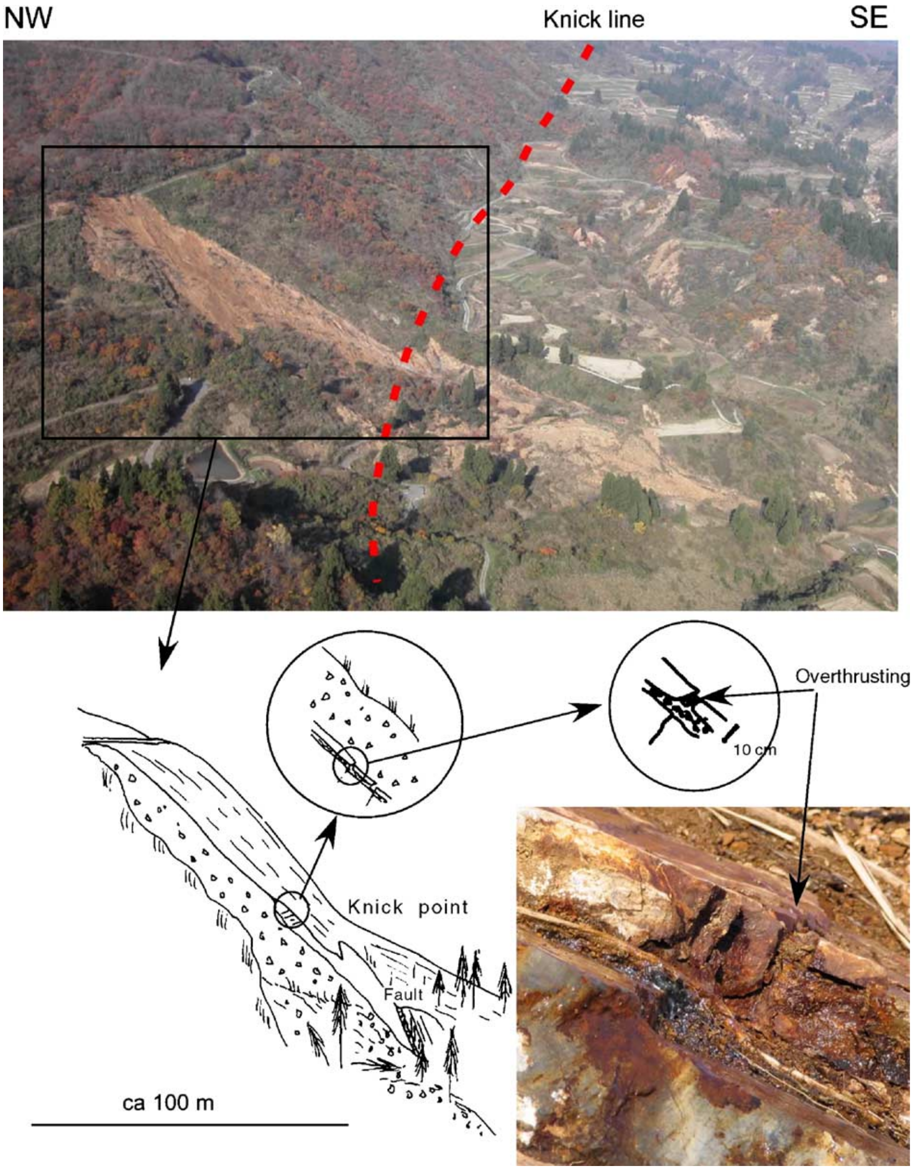

Fig. 14. Kazekuchitoge slide evolved from buckling in the lower part of the slope. Aerial photographs, schematic sketches, and a close-up view of the overthrusting.

new landslides. All of the investigated major landslides except for one, which was proceeded by buckling, were undercut by erosion or artificial cutting (Table 2). Exactly the same undercutting condition was also found for the catastrophic landslides at the 1978 Izu-Oshima-Kinkai earthquake in central Japan. That earthquake triggered at least seven long run-out landslides in pyroclastic fall deposits with sliding surfaces in a paleozol: six of them were new landslides and were undercut by erosion or artificial cutting, and the seventh was preceded by creep movement and buckling (Chigira, 1982). Therefore, although the infinite slope analysis has been used for shallow, slope-parallel beds, the undercutting condition needs to be incorporated into stability analyses. The importance of undercutting was pointed out by Keefer (1984a,b) from the literature on landslides triggered by earthquakes. Buckling could be dealt with in a similar way as undercutting. Landslides preceded by buckling occurred during the 1999 Chi-Chi earthquake on a much larger scale (Wang et al., 2003a). The Higashiyama hills seem to have been experiencing many landslides caused by earthquakes and rainfall. In consideration of the iteration of the landslide and undercutting erosion, a long-term analysis which includes

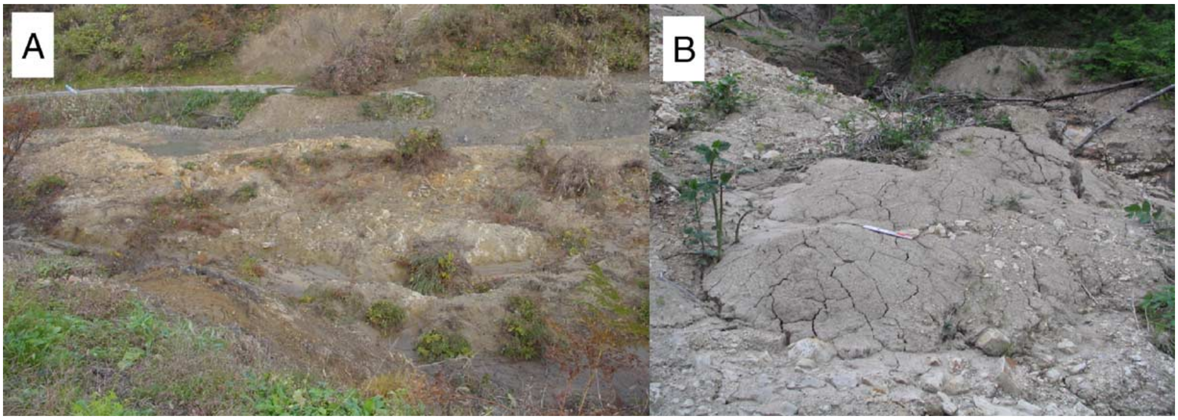

Fig. 15. Mobilized valley fill (A, West of Jyunihira, photo taken on November 8th in 2004) and muddy sand blows on a mobilized fill (B, northeast of Uragara in Fig. 2, photo taken on May 2nd in 2005). In picture A, one-lane road is seen on the opposite side of the valley bottom and water forms a pond on the middle right of the mobilized fill. The scale in the center of picture B is 30 cm.

the global-sea level change and tectonic uplift must be conducted.

Most of the catastrophic landslides triggered by the Mid Niigta prefecture earthquake, which we investigated, had sliding surfaces along the planar bedding planes or near the oxidation front which is nearly slope-parallel in general (Chigira, 1990). This earthquake also induced landslides that probably have circular sliding surfaces, but most of them had rather small displacements, forming only small cracks or scarplets. This difference might be related to the earthquake shaking, which is cyclic loading rather than static loading. Many of the catastrophic landslides triggered by other earthquakes also had planar sliding surfaces, including the Tsaoling and Chiu-fen-erh-shan landslides (Chigira et al., 2003; Wang et al., 2003a) and other relatively small slides (Central Geological Survey, 2000) triggered by the 1999 Chi-Chi earthquake, the Bairaman slide (King et al., 1989), the Ontake slide (Endo et al., 1989; Voight and Sousa, 1994), landslides by the 1978 Izu-Oshima-Kinkai earthquake (Chigira, 1982), and landslides in Anchorage by the 196 Alaska earthquake (Hansen, 1965; Seed and Wilson, 1967). However, there have also been reports of landslides with circular or curved sliding surfaces being triggered by earthquakes, so it may be more accurate to state that landslides with planar sliding surfaces tend to be transformed to catastrophic or highly mobile landslides by earthquakes.

Planar sliding surfaces make characteristic surface morphologies, like ridges and grabens and "roll-over antiforms," as was seen in the Mid Niigta prefecture earthquake (Fig. 17). Additional study is necessary to understand what factors determine the type of deformation and surface morphology of translational landslides with a planar sliding surface.

The ratio of the elevation difference from he top of the scar to the tip of the deposit divided by the horizontal projection of the distance between these two points (H/L) was called Fahrböschung by Heim (1932), and has been used as an index for the mobility of landslides. It was considered an "equivalent coefficient of friction" by Shreve (1968). Many data on the equivalent coefficient of friction have been compiled, and show a trend of decreasing coefficient with increasing volume for rock avalanche (Hsu, 1975; Scheidegger, 1973). However, it has not been examined whether the equivalent coefficients of friction change according to the materials involved.

Fig. 18 shows the apparent friction angles, which are $\tan^{1}(H/L)$, obtained from mobile landslides triggered by previous earthquakes in Japan and the Mid Niigta prefecture earthquake. Referred earthquakes include the 1968 Tokachi-oki (Inoue et al., 1970), 1978 Izu-Oshima-Kinkai (Chigira, 1982), the 1984 Nagano-ken-Seibu (Okuda et al., 1984), the 1995 Hyogo-ken-Nanbu (Sassa and Fukuoka, 1995), and the 2003 Miyagi-ken-Nanbu earthquakes (Miyagi et al., 2004). The landslides triggered by earthquakes in Japan used to be mostly new ones before the Mid Niigta prefecture earthquake, and occurred mainly on pyroclastic slopes or water-saturated man-made fill; many of them showed high mobility, as is seen in Fig. 18. However, even apparently mobile landslides and new landslides triggered by the Mid Niigta prefecture earthquake, except for the mobilized valley fill, had rather larger apparent friction angles than the previous landslides by earthquakes. This difference may be attributed to the difference in the materials, the extent of saturation, and whether the landslides were new or reactivated ones. In contrast, the average longitudinal slopes of valleys, where sediment mobilization occurred, were smaller and close to the apparent friction angles of landslides triggered by previous earthquakes (Fig. 18). This may be due to the fact that the mobilized sediments were saturated, which was confirmed in several locations, and partial liquefaction may possibly have occurred.

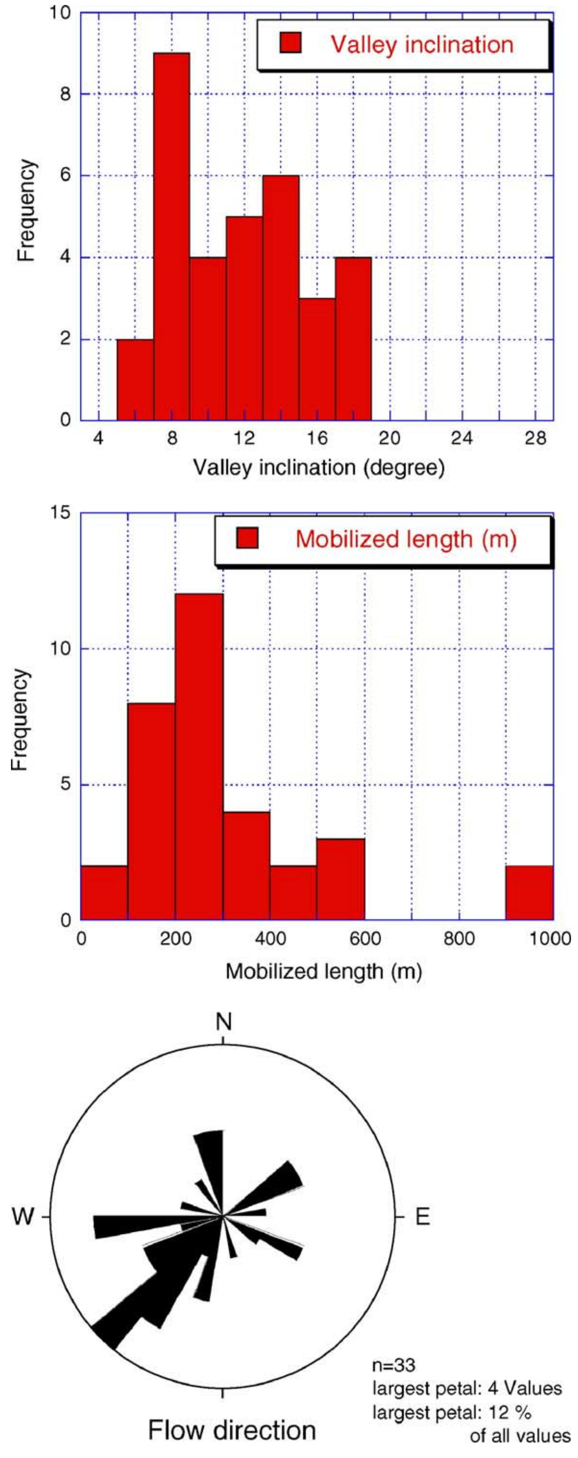

Fig. 16. Geometrical data of mobilized valley fill (valley inclination, mobilized intervals, and directions).

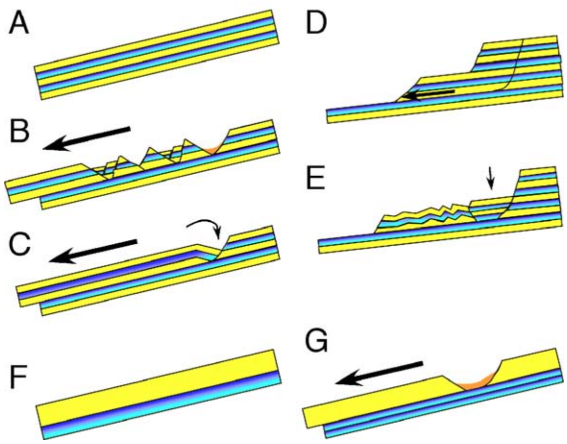

Fig. 17. Schematic sketches showing the landforms and internal structures made by landslides with a planar sliding surface parallel to the bedding plane. A: Alternating beds of sandstone and siltstone with a smooth ground surface; B: Rockslide of alternating beds of sandstone and siltstone, forming “ridges and grabens”; C: Rockslide of alternating beds of sandstone and siltstone, forming a “roll-over anticline” on the listric part of the sliding surface; D and E: Rockslide of alternating beds of sandstone and siltstone by lateral spreading and settlement. F and G: Rockslide of sandstone on a siltstone bed, leaving a depression filled with debris.

5. Conclusions

The 2004 Mid Niigta prefecture earthquake (M 6.8) triggered more than a thousand of landslides in areas underlain by Miocene to Quaternary-aged sedimentary rocks. The most common landslides were shallow disrupted landslides on steep slopes, but deep landslides also occurred in many locations. We studied about 100 deep landslides by field investigation and by interpreting aerial photographs. The results showed that many of these landslides occurred due to the reactivation of previously existing landslides and the mobilization of valley bottom sediments. Except for the mobilization of valley bottom sediments, these landslides had planar sliding surfaces along bedding planes or along the oxidation front. The bedding-parallel sliding surfaces were made at the boundary between the overlying sandstone and underlying siltstone or along the bedding planes between alternating beds of sandstone and siltstone. Sliding surfaces along the oxidation front occurred in the area of black mudstone. New landslides (rockslide-avalanches) occurred with sliding surfaces in several-cm-thick tuff intercalated in siltstone. Most of the deep landslides occurred on slopes undercut by

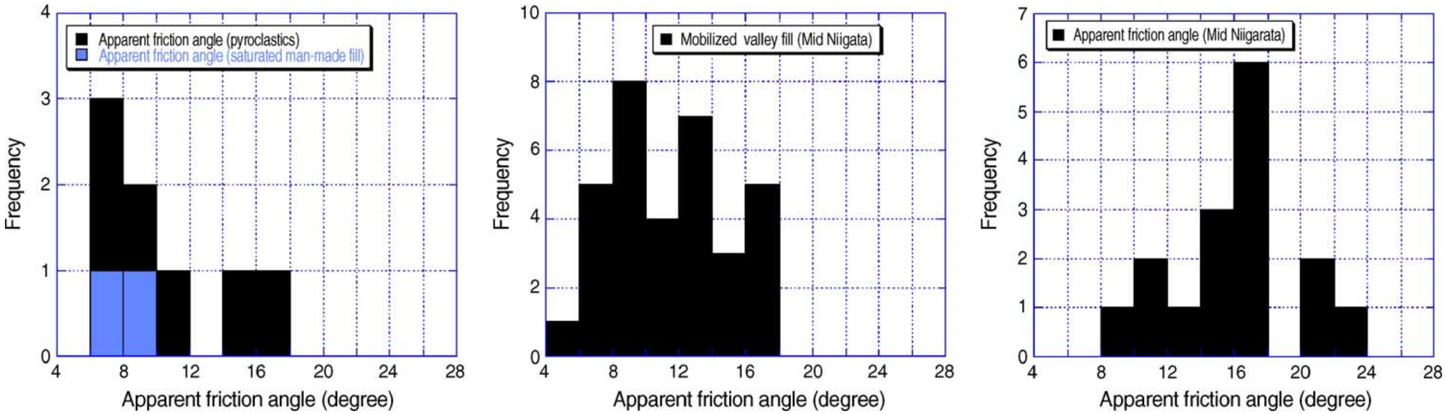

Fig. 18. Apparent friction angles of landslides induced by previous earthquakes in Japan (left), landslides induced by the 2004 Mid Niigta prefecture earthquake (right), and the longitudinal angle of valleys mobilized by the Mid Niigta prefecture earthquake (center).

erosion or artificial excavation. One rockslide-avalanche occurred on a slope where buckling deformation preceded the earthquake. Gentle valley bottom sediments were mobilized in about 30 locations, probably because they were saturated and partial liquefaction occurred as a result of the earthquake.

Acknowledgments

We are very grateful to the following researchers for their discussions with us in the field and in the laboratory. Yamagishi, H. and Watanabe, N. of Niigata University; Nakasuji, A., Ohzu, K., Sudou, H., Fukui, K., and Tanase, T. of the Japan Society of Engineering Geology; Sekiguchi, T. and Sato, P. H. of the Geographical Survey Institute; Sassa, K. and Fukuoka, H. of Kyoto University; Ochiai, H. and Okada, Y. of the Forestry and Forest Products Research Institute; and Yamasaki, T. of the Japan Conservation Engineers Co. We are also grateful to Nagashima, T., the former mayor of Yamakoshi Village, who allowed us to enter the evacuated village. This research was supported by a Special Coordinating Fund for Promoting Science and Technology of the Ministry of Education, Culture, Sports, Science and Technology of Japan.

References

Central Geological Survey (Republic of China), 2000. Landslide disasters of Taiwan. Geohazard Report. Central Geological Survey, MOEA, Taiwan, Taipei. 145 pp.

Chigira, M., 1982. Dry debris flow of pyroclastic fall deposits triggered by the 1978 Izu-Oshima-Kinkai earthquake: the “collapsing” landslide at Nanamawari, Mitaka-Iriya, southern Izu Peninsula. Journal of Natural Disaster Science 4, 1–32.

Chigira, M., 1990. A mechanism of chemical weathering of mudstone in a mountainous area. Engineering Geology 29, 119–138.

Chigira, M., Wang, W.-N., Furuya, T., Kamai, T., 2003. Geological causes and geomorphological precursors of theTsaoling landslide triggered by the 1999 Chi-Chi Earthquake, Taiwan. Engineering Geology 68, 259–273.

Endo, K., Sumita, M., Machida, M., Furuichi, M., 1989. The 1984 collapse and debris avalanche deposits of Ontake Volcano, central Japan. In: Latter, J.H. (Ed.), IAVCEI Proceedings in Volcanology. Springer, pp. 210–229.

Hadley, J.B., 1964. Landslides and related phenomena accompanying the Hebgen Lake earthquake of August 17, 1959. U.S. Geological Survey Professional paper 435, 107–138.

Hansen, W.R., 1965. Effects of the earthquake of March 27, 1964 at Ancourage, Alaska. U.S. Geological Survey Professional paper 542A, 68.

Harp, E.L., Jibson, R.W., 1996. Landslides triggered by the 1994 Northridge, California earthquake. Bulletin of the Seismological Society of America 86, 319–332.

Heim, A., 1932. Bergsturz und Menschenleben. Fretz und Wasmuth, Zurich.

Hsu, K.J., 1975. Catastrophic debris streams (sturzstroms) generated by rockfalls. Geological Society of America Bulletin 86, 129–140.

Inoue, Y., Honsho, S., Matsushima, M., Esashi, Y., 1970. Geological and soil mechanical studies on the slides occurred during the 1968 Toakachioki earthquake in southeastern area of Aomori Prefecture. Report, vol. 69086. Central Research Institute of Electric Power Industry, pp. 1–27.

Japan Geographical Institute, 2004. Earthquake hazards map by the 2004 Mid-Niigata prefecture earthquake.

Jibson, R.W., Harp, E.L., Michael, J.A., 2000. A method for producing digital probabilistic seismic landslid hazard maps. Engineering Geology 58, 271–290.

Keefer, D., 1984a. Landslides caused by earthquakes. Geological Society of America Bulletin 95, 406–421.

Keefer, D., 1984b. Rock avalanches caused by earthquakes: source characteristics. Science 223, 1288–1290.

Keefer, D.V., 2000. Statistical analysis of an earthquake-induced landslide distribution — the 1989 Loma Prieta, California event. Engineering Geology 58, 231–249.

Keefer, D.K., Manson, N.W., 1998. Regional distribution and characteristics of landslides generated by the earthquake. U.S. Geological Survey Professional paper 1551C, C7–C32.

King, J., Loveday, I., Schuster, R.L., 1989. The 1985 Bairaman landslide dam and resulting debris flow, Papua New Guinea. Quarterly Journal of Engineering Eeology 105, 257–270.

Kobayashi, T., 1987. Geological aspect of the 1984 Denjo landslide on Ontake Volcano. Transactions, Japanese Geomorphological Union 8 (2), 113–125.

Kobayashi, I., Tateishi, M., Yoshioka, T., Shimazu, M., 1991. Geology of the Nagaoka District. Geological Survey of Japan, Quadrangle Series (Scale 1:50,000) Niigata (7) No. 38.

Miyagi, T., Inspection committee of the Japan Landslide Society, and Inspection committee of the APERIF, 2004. A report of the landslide disaster activated at Tsukidate Miyagi prefecture by the Sanriku-minami earthquake, 26 May, 2003. Journal of the Japan Landslide Society 40 (2), 45–46.

Newmark, N.M., 1965. Effects of earthquakes on dams and embankments. Geotechnique 15 (2), 139–160.

Okuda, S., Okunishi, S., Suwa, K., Yokoyama, H., Yoshioka, K., 1984. Restoration of motion of debris avalanche at Mt. Ontake in 1984 and some discussions on its moving state. Annual Report of the Disaster Prevention Research Institute, Kyoto University, vol. 28, pp. 491–504.

Parise, M., Jibson, R.W., 2000. A seismic landslide susceptibility rating of geologic units based on analysis of characteristics of landslides triggered by the 17 January, 1994 Northridge, California earthquake. Engineering Geology 58, 251–270.

Plafker, G., Ericksen, G.E., Fernandez, C.J., 1971. Geological aspects of the May 31, 1970, Peru Earthquake. Bulletin of the Seismological Society of America 61, 543–578.

Ramsay, J.G., Huber, M.I., 1987. Folds and fractures. The Techniques of Modern Structural Geology, vol. 2. Academic press, London.

Research Group for Active Faults of Japan (Ed.), 1991. Active Faults in Japan: Sheet Maps and Inventories (Revised edition). Tokyo University Press, Tokyo. 437 pp.

Rodriguez, C.E., Bommer, J.J., Chandler, R.J., 1999. Earthquake-induced landslides: 1980–1997. Soil Dynamics and Earthquake Engineering 18, 325–346.

Sassa, K., Fukuoka, H., 1995. Nikawa landslide and the prediction of earthquake-induced landslides. In: Japan Landslide Society (Ed.), Report on the landslides and slope failures triggered by the

Hyogoken-Nanbu earthquake and other earthquakes. Japan Landslide Society, Tokyo, pp. 145–170.

Sato, H., Sekiguchi, T., Kojirai, R., 2004. Relationship between landslide distribution and geology, geomorphology, and epicenters. In: Sassa, K. (Ed.), Symposium on landslide hazards by the 2004 Mid Niigta prefecture Earthquake, Special Coordinating Fund for Promoting Science and Technology of the Ministry of Education, Culture, Sports, Science and Technology of Japan, Tokyo, pp. 7–15.

Scheidegger, A.E., 1973. On the prediction of the reach and velocity of catastrophic landslides. Rock Mechanics 5, 231–236.

Seed, H.B., Wilson, S.D., 1967. The Turnagain Heights landslide, Anchorage, Alaska. Journal of the Soil Mechanics and Foundations Division, Proceedings of the American Society of Civil, pp. 325–353.

Shreve, R.L., 1968. The Blackhawk landslide. Special Paper, vol. 108. Geological Society of America, p. 47.

The Geographical Survey Institute, 2004. A map of the disasters caused by the Mid Niigta prefecture Earthquake. The Geographical Survey Institute, Japan. 1 sheet with a scale of 1:30,000.

Voight, B., Sousa, J., 1994. Lessons from Ontake-san: a comparative analysis of debris avalanche dynamics. Engineering Geology 38, 261–297.

Wang, W.N., Nakamura, H., Tsuchiya, S., Chen, C.C., 2002. Distributions of landslides triggered by the Chi-Chi earthquake in Central Taiwan on September 21, 1999. Journal of the Japan Landslide Society 38 (4), 318–326.

Wang, W.-N., Furuya, T., Chigira, M., 2003a. Geomorphological precursors of the Chiu-fen-erh-shan landslide triggered by the Chi-chi earthquake in Central Taiwan. Engineering Geology 69, 1–13.

Wang, W.N., Wu, H.L., Nakamura, H., Wu, S.C., Ouyang, S., Yu, M.F., 2003b. Mass movements caused by recent tectonic activity: the 1999 Chi-Chi earthquake in central Taiwan. The Island Arc 12, 325–334.

Wilson, R.C., Keefer, D.K., 1983. Dynamic analysis of a failure from the 6 August 1979 Coyote Lake, California earthquake. Bulletin of the Seismological Society of America 73, 863–877.

Yagi, H., Yamazaki, T., Moriiwa, T., 2004. Distribution map of landslides triggered by the 2004 Chuetsu earthquake, Japan Conservation Engineers, Tokyo.

Yanagisawa, Y., Kobayashi, I., Takeuchi, K. Tateishi, M. Chihara, K., Kato, H., 1986. Geology of the Ojiya District. Geological Survey of Japan, Quadrangle Series (Scale 1:50,000) Niigata (7) No. 50.